Elevated leptin disrupts epithelial polarity and promotes premalignant alterations in the mammary gland

Iliana Tenvooren[1,#], **Mónica Z. Jenks**[1,#], **Hamza Rashid**[1], **Katherine L. Cook**[2,10], **Joëlle K. Muhlemann**[3], **Christopher Sistrunk**[4], **Julia Holmes**[1], **Kevin Wang**[5], **Keith Bonin**[5], **Kurt Hodges**[6], **Hui-Wen Lo**[1], **Ayaz Shaikh**[7], **Ignacio G. Camarillo**[8], **Sophie A. Lelièvre**[9], **Victoria Seewaldt**[4], and **Pierre-Alexandre Vidi**[1,10,*]

[1]Department of Cancer Biology, Wake Forest School of Medicine, Winston-Salem, NC 27157, USA.

[2]Department of Surgery, Wake Forest School of Medicine, Winston-Salem, NC 27157, USA.

[3]Department of Biology, Wake Forest University, Winston-Salem, NC 27109, USA.

[4]Department of Population Sciences, City of Hope, Duarte, CA 91010, USA.

[5]Department of Physics, Wake Forest University, Winston-Salem, NC 27109, USA.

[6]Department of Pathology and Laboratory Medicine, University of Cincinnati, Cincinnati, OH 45219, USA.

[7]Indiana University School of Medicine, IU Health Arnett Hospital, Lafayette, IN 47905, USA.

[8]Department of Biological Sciences, Purdue University, West Lafayette, IN 47907, USA.

[9]Department of Basic Medical Sciences, Purdue University, West Lafayette, IN 47907, USA.

[10]Comprehensive Cancer Center of Wake Forest University

Abstract

Obesity is a highly prevalent and modifiable breast cancer risk factor. While the role of obesity in fueling breast cancer progression is well established, the mechanisms linking obesity to breast cancer initiation are poorly understood. A hallmark of breast cancer initiation is the disruption of apical polarity in mammary glands. Here we show that mice with diet-induced obesity display mislocalization of Par3, a regulator of cellular junctional complexes defining mammary epithelial polarity. We found that epithelial polarity loss also occurs in a 3D coculture system that combines acini with human mammary adipose tissue, and establish that a paracrine effect of the tissue adipokine leptin causes loss of polarity by overactivation of the PI3K/Akt pathway. Leptin sensitizes non-neoplastic cells to proliferative stimuli, causes mitotic spindle misalignment, and

Address for correspondence: Pierre-Alexandre Vidi, Department of Cancer Biology, Wake Forest School of Medicine, Winston-Salem, NC 27157, USA; phone (336) 716 7122; pvidi@wakehealth.edu.
#Equal contribution

expands the pool of cells with stem/progenitor characteristics, which are early steps for cancer initiation. We also found that normal breast tissue samples with high leptin/adiponectin transcript ratio characteristic of obesity have an altered distribution of apical polarity markers. This effect is associated with increased epithelial cell layers. Our results provide a molecular basis for early alterations in epithelial architecture during obesity-mediated cancer initiation.

Introduction

Obesity is one of the few preventable cancer risk factors in the breast and other organs [1, 2]. While obesity is a well-established driver of cancer progression, the mechanisms by which obesity facilitates breast cancer initiation in postmenopausal [3] and in high-risk pre-menopausal [4] women are poorly understood. Elevated estrogen production by adipocytes may contribute to the increased post-menopausal risk for estrogen receptor (ER)-positive tumors. However, obesity also increases the risk for triple-negative breast cancers (TNBC) that lack ER expression [5], suggesting that additional mechanisms linked to obesity are driving cancer initiation.

Multiple factors are deregulated in obesity, including the balance between levels of leptin and adiponectin, which are mediators of cancer initiation and progression [6, 7]. Whereas adiponectin levels are inversely proportional to BMI and to breast cancer risk, leptin serum levels are elevated 2–5 fold in obese vs. lean individuals [8, 9], as well as in animal models of obesity [10]. In breast cancer cell lines, leptin stimulates proliferation, angiogenesis, migration, and metastasis by activating the oncogenic STAT3, ERK and PI3K/Akt pathways [6]. While these oncogenic effects are typically not measured in pre-neoplastic cell models, the role of leptin in cancer initiation is supported by epidemiological studies showing that circulating leptin levels are elevated in women with pre-malignant breast disease compared to controls [11]. Interestingly, increased breast cancer risk associated with high leptin persists after adjusting for waist circumference (used as an index for obesity), which indicates a direct contribution of leptin to breast cancer initiation [12]. However, the mechanisms by which leptin increases cancer risk have not been clearly established.

Disruption of tissue polarity is one of the first identifiable events in the initiation of carcinoma [13–15]. Apical-basal polarity is defined by the structural and functional organization of cellular components relative to the lumen and basement membrane. Apical cell membranes in the mammary gland delineate the luminal space and are segregated from basolateral membranes by tight junctions (TJ). These junctions, together with adherens junctions (AJ), establish a seal ensuring cohesion of the epithelium. Cell-cell junctions function as gates for selective diffusion between cells and between basal and luminal interstitial spaces, and tether the actomyosin cytoskeleton. Several polarity proteins localize at cell-cell junctions as well as in the cytosol and the nucleus where they regulate signaling, gene expression, and genome maintenance [16–18]. Alteration of cell polarity leads to misregulation of proliferative and survival pathways by shifting the equilibrium between these distinct cytosolic and nuclear pools. Polarity complexes also regulate mitotic spindle orientation and hence cell division within the epithelial plane to prevent cell multilayering. Moreover, polarity prevents cell cycle entry [19] and is essential for efficient DNA repair in

mammary epithelial cells [20]. As a corollary, disruption of polarity may promote cancer initiation in the breast and other organs. It is currently unknown if and how obesity and its associated metabolic dysfunction deregulate polarity systems. Here, we tested the hypothesis that obesity-associated alterations in adipokine levels negatively affect epithelial polarity.

Results

The polarity protein Par3 is mislocalized in the mammary gland of a mouse model of obesity

To assess the impact of obesity on epithelial polarity in the mammary gland, we first used a mouse model of diet-induced obesity (DIO) [21] (Fig. 1a). Mammary glands were collected from the animals at 20 weeks of age, which corresponds to the reproductive, premenopausal stage of humans, in order to analyze the localization of the polarity protein Par3. This protein regulates apical and basal cell membrane territories and localizes predominantly to TJ in differentiated epithelia [22]. Moreover, Par3 depletion was shown to promote tumorigenesis in mice [23]. In mice fed a control diet, apical Par3 signal was detected in 50% of acini and ducts, whereas only 36% of mammary epithelial structures of DIO mice had apical Par3, which was reflected by a significantly lower polarity score (Fig. 1b).

A paracrine effect from adipose tissue alters apical polarity

To further understand how obesity may compromise breast epithelial polarity, we cocultured breast epithelial cells and adipose tissue explants derived from breast reduction mammoplasties (Supplementary Fig. S1). In 3D culture, non-neoplastic HMT-3522 S1 mammary epithelial cells arrest proliferation and differentiate into acini that establish and maintain apical TJ - a hallmark of epithelial polarity - around their small lumina [24, 25]. Confocal microscopy analysis of acini immunostained for the TJ marker ZO-1 revealed a strong decrease in apical localization of this polarity marker in acini cocultured with adipose tissue explants (Fig. 1c). To discriminate between direct effects through cell-cell contacts or indirect effects via the action of soluble factors, conditioned media were prepared from adipose tissue explants of different patients. Treatments of differentiated S1 acini with conditioned media decreased the proportion of structures with apical ZO-1 relative to controls (Fig. 1d-f). The result suggests that a paracrine effect causes the loss of apical marker localization in breast acini.

Leptin in mammary tissue increases with overweight and obesity

The adipokine leptin is a well-characterized oncogenic factor secreted by adipose tissue. Circulating levels of leptin positively correlate with BMI, and leptin concentration measured in our conditioned media (57.4 ± 24.1 ng/ml) was within the range of values measured in serum from obese individuals [8]. However, leptin's oncogenic effects in the breast are likely determined by the local interstitial concentration of the adipokine in the mammary epithelial microenvironment, rather than circulating levels. We therefore quantified breast tissue levels from a panel of adipokines, cytokines, and growth factors in surgical excision specimens from women at high risk for breast cancer [26] (Table 1). We did not detect changes in levels of adiponectin, insulin, MCP1, and IL-8, previously reported to be associated with obesity [9, 27, 28]. This discrepancy may be explained by the fact that circulating rather than tissue

levels were measured in most previous studies and by the relatively small size of our cohort. Leptin levels significantly correlated with BMI in our cohort, which highlights the importance of tissue leptin in the context of obesity and encouraged us to focus on this adipokine for further *in vitro* studies.

Leptin signals disrupt apical-basal polarity

Leptin levels positively correlate with breast cancer risk and with BMI in humans [8]. We also measured increased leptin abundance and elevated *Lep* gene expression in mammary glands from DIO mice compared to mice on the control diet (Supplementary Fig. S2). The mechanisms by which leptin promotes carcinogenesis are incompletely understood and we hypothesized that excessive leptin signaling might contribute to the disruption of polarity markers measured in human and mice acini. In agreement with this hypothesis, a specific leptin receptor (LEPR) antagonist (LA) partially restored apical localization of ZO-1 in acini treated with fat-conditioned media (Fig. 1e). Similarly, leptin neutralization with leptin-specific antibodies significantly improved apical ZO-1 localization in cells treated with fat-conditioned media (Fig. 1f).

Next, we analyzed apical polarization of acini treated with levels of purified adipokines typical for lean conditions (low leptin and high adiponectin) or with high leptin/low adiponectin levels typical for obesity. Whereas the apical ZO-1 marker was not altered in acini treated with the 'lean' adipokine ratio compared to untreated controls, exposure to high leptin/low adiponectin led to reduced apical ZO-1 localization (Fig. 2a). Leptin alone was sufficient to disrupt the apical distribution of ZO-1 and the integral TJ protein claudin-1 in differentiated acini, and this effect was reverted by a LEPR antagonist (Fig. 2b-c). The same effect of leptin on TJ was measured in 3D cultures of non-immortalized post-stasis human mammary epithelial cells (psHMEC) (Supplementary Fig. S3a-b).

For validation of our visual assessment of polarity marker distribution, we developed a computational image analysis approach to quantify apical polarity in microscopy images based on radial signal distribution. The software identifies acini based on a nuclear stain and computes normalized radial profiles of polarity markers (Supplementary Fig. S3c-d). Radial profile analyses of ZO-1 distribution confirmed loss of apical polarity by leptin (Fig. 2d).

The function of apical cell-cell junctions depends on the cortical actin cytoskeleton that organizes into perijunctional actomyosin rings stabilizing junctional complexes. The TJ scaffold protein ZO-1 directly binds F-actin and regulates the arrangement and activity of the cortical cytoskeleton. Bright F-actin staining at the apical plasma membrane was significantly reduced by leptin treatment (Fig. 2e). Silencing LEPR expression with either siRNA or shRNA abolished leptin's effect on cortical actin, further indicating that canonical LEPR signaling mediates leptin's effect on cell polarity (Fig. 2e). We also measured a 40% decrease of apical Par3 localization in leptin-treated acini compared to vehicle (Fig. 2f), which parallels our initial observation in the DIO mouse model.

Acini were analyzed by transmission electron microscopy (TEM) to further assess the effect of leptin on epithelial junctional complexes. TJ were apparent at cell-cell junctions, but their low contrast led to poor concordance between independent investigators for their systematic

identification. Unlike TJ, AJ/desmosomes were clearly identified and quantified in TEM images. Acini exposed to leptin had significantly less junctions and the radial distribution of the junctions was shifted towards the basal side of the acini (Supplementary Fig. S4a-c). Reduced apical AJ localization after leptin treatment was confirmed by immunostaining for E-cadherin and β-catenin (Supplementary Fig. S4d).

A key role of TJs is to establish a barrier that limits paracellular diffusion of ions and macromolecules. To test whether leptin-mediated loss of apical polarity affects this barrier function, we measured the diffusion of Evans blue-labeled albumin (EBA) across a monolayer of S1 cells. EBA permeability was significantly increased in acini exposed to leptin compared to vehicle, and this effect was reverted by the LEPR antagonist (Fig. 2g). Together, the results show that leptin signaling in mammary acini disrupts apical polarization as well as the function of cell-cell junctional complexes.

Loss of apical polarity by leptin is mediated by PI3K/Akt

Leptin binding to LEPR activates the signal transducer and activator of transcription 3 (STAT3), the mitogen-activated protein kinase (MAPK), and the phosphatidylinositol 3 kinase (PI3K) pathways [6]. To elucidate the mechanism of polarity loss by leptin, we blocked these pathways in acini. Inhibition of STAT3 or MAPK did not prevent leptin-mediated polarity loss and we did not detect STAT3 nor MAPK phosphorylation in S1 cells treated with leptin (Supplementary Fig. S5). In contrast, pharmacological inhibition of PI3K with LY294002 or wortmannin completely eliminated leptin's effect on apical polarity (Fig. 3a). Treatment with the Akt inhibitor MK2206 also prevented apical polarity loss by leptin (Fig. 3b). Western blot analysis of S1 monolayer extracts and immunostaining of S1 acini confirmed Akt phosphorylation by both acute and prolonged leptin treatments and validated the inhibitor treatments (Fig. 3c-d). Moreover, ectopic expression of constitutively activated Akt (T308D/S473D; CA-Akt [29]) in S1 acini significantly reduced the proportion of structures with apical ZO-1 signals (Fig. 3e). Note that the measured 20% decrease in apical polarity underestimated the effect of CA-Akt, because S1 transfection efficiency was ~30%. We therefore conclude that, in our model system, the LEPR/PI3K/Akt signaling axis compromises tissue architecture when overstimulated. This result is consistent with our previous observation by proteomic profiling that Akt is frequently activated in normal breast tissue from obese women [26].

Leptin causes depolarization of afadin, an Akt substrate required for establishment and maintenance of cell polarity

Afadin/MLLT4 is an Akt substrate [30] regulating TJ and AJ formation [31, 32]. Accordingly, most S1 acini displayed apical afadin staining, overlapping with the TJ marker claudin-1 (Fig. 4a). Leptin disrupted apical polarization of afadin (Fig. 4a) and increased afadin phosphorylation (S1718; Akt substrate; Fig. 4b), consistent with afadin disengagement from apical junctional complexes upon phosphorylation [30]. As expected, afadin silencing in S1 acini impaired apical polarization of the structures (Fig. 4c). To determine if afadin is also necessary for the maintenance of polarity, differentiated acini were briefly permeabilized and incubated with antibodies against afadin or GFP as control. The permeabilized afadin antibodies bound to apical structures in the majority of the acini.

Incubation with these antibodies led to reduced apical claudin-1 localization compared to controls (Fig. 4d), suggesting that afadin regulates TJ maintenance. Hence, loss of afadin at cell-cell junctions by leptin may cause loss of epithelial polarity.

Leptin sensitizes acini to growth factors

Leptin had no direct effect on S1 acini proliferation: similar to vehicle-treated cells, S1 acini exposed to leptin levels that disrupt apical polarity remained in proliferation arrest (i.e. Ki67-negative) and retained similar sizes (Fig. 5a-c), and leptin did not alter cell cycle distribution (Supplementary Fig. S6a). These results were expected since other groups have shown that leptin does not induce proliferation in pre-malignant mammary epithelial cells [33]. Similarly, whereas multiple studies have shown that leptin promotes migration and invasion in cancer cells [34], treatment of S1 and psHMEC non-neoplastic cells did not promote single-cell and collective migration (Supplementary Fig. S6b-c), nor lead to cell invasion or invasive protrusion in Matrigel (Supplementary Fig. S6d). High leptin in obesity is often concomitant with increased levels of several other growth factors, including insulin and IGF-1 [7]. These factors may act synergistically with leptin during cancer initiation and progression. As shown in Fig. 5b, treatment of differentiated acini with leptin in combination with IGF-1 and insulin at levels found in obesity, lead to cell cycle reentry (Ki67-positive cells). We also measured increased acini sizes in the combined treatment (Fig. 5c). Importantly, insulin and IGF-1 did not induce proliferation in the absence of leptin. Immunostaining for ZO-1 confirmed loss of apical polarity for acini treated with leptin, as well as in acini treated with leptin combined with insulin and IGF-1, but not for acini treated with IGF-1 and insulin (Fig. 5d). Two nonmutually exclusive mechanisms may account for our observations: Leptin, insulin, and IGF-1 may act synergistically at the levels of the receptors and/or loss of apical polarity by leptin may alter the integration of proliferative signals from the microenvironment. To distinguish between these two possibilities, we first examined the polarity status of Ki67-positive acini (defined as structures with   2 nuclei stained with Ki67) in the combined treatment. Whereas the overall proportion of apically polarized structures was 40% in this treatment, only 25% of Ki67-positive acini were polarized, suggesting a link between polarity loss and proliferation. To further test this relationship, we temporally dissociated the treatments with leptin and the growth factors. Acini were first exposed to vehicle or leptin for 72h, leading to polarity loss in the leptin treatment. Then acini were washed and treated with either vehicle or insulin and IGF-1. Sequential exposure to leptin and growth factors increased the proportion of Ki67-positive acini compared to the single treatments and to vehicle (Fig. 5e). This result was similar to that of the combined treatment, albeit with a decreased amplitude. Although we do not exclude synergies between LEPR and other growth factor receptors leading to proliferation, the results suggest that loss of apical polarity *per se* sensitizes acini to proliferative stimuli.

Leptin leads to mitotic spindle misalignment and cell multilayering

Maintenance of a single layer of cells in the mammary gland and other simple epithelia requires orientation of the mitotic spindle poles parallel to the basement membrane. In contrast, perpendicular or random spindle orientation can lead to cell multilayering, an important stage of cancer initiation. The PAR polarity system (Par3, Par6, aPKC, and

CDC42) defines mitotic spindle orientation by regulating the localization of the $G\alpha_i$/LGN/ NuMA complex that tethers spindle poles at the plasma membrane [35]. In simple epithelia, PAR ensures that $G\alpha_i$/LGN/NuMA is targeted to the lateral cell membranes, thereby promoting cell divisions parallel to the basement membrane. Accordingly, loss of Par3 expression leads to spindle misorientation in MDCK cells [36]. Afadin was also shown to promote planar cell divisions by anchoring LGN to lateral membranes [37]. Since mammary cells exposed to leptin have mislocalized Par3 (Fig. 2f) and afadin (Fig. 4a), leptin may impact the orientation of breast epithelial cell divisions. To determine if loss of epithelial polarity by leptin alters mitotic spindle orientation, S1 cells were cultured on laminin-coated coverslips to produce monolayers with apical-basal polarity [38]. Spindle poles were labeled by immunostaining for NuMA and the angle between the spindle axis and the basement membrane was measured in confocal datasets. In these experiments, leptin treatment resulted in increased and significantly more variable (F test of variance, $P = 0.0002$) spindle pole angles compared to vehicle-treated cells (Fig. 6a-b). Despite the misoriented spindle axes, we did not observe multilayering in our assay, likely due to active anoikis in the anchorage-dependent S1 cells.

Analysis of mammary gland tissue from obese and lean mice revealed an increased proportion of hyperplasia (defined as at least three cell layers) in DIO animals ($16\% \pm 2\%$ vs. $20\% \pm 5\%$ for control and OID, respectively; Fig. 6c). Moreover, apical polarity negatively correlated with hyperplasia (Fig. 6d), suggesting that loss of polarity may cause epithelial multilayering in a tissue context.

Misorientation of the mitotic spindle poles in simple epithelia may lead to the expansion of the pool of stem/progenitor cells [15]. Accordingly, we found that S1 acini exposed to elevated leptin have an increased proportion of cells with stem/progenitor characteristics (Supplementary Fig. S6e-f), which confirms a previous report [39] showing that the proportion of breast epithelial cells with stem-like properties correlates with leptin levels in normal breast tissue samples.

Reduced apical polarity in normal breast tissue is associated with multilayering and with adipokine imabalance

We assessed apical polarity in normal breast tissue from reduction mammoplasties and mastectomies by quantifying the localization of ZO-1, Par3, and cortical actin (Fig. 7a and Supplementary Fig. S7a). No significant difference in marker localization was measured between the two different sources of tissue, although apical polarity scores tended to be lower in mastectomy compared to reduction mammoplasty samples (Supplementary Fig. S7b). Concordance between the different apical polarity markers was high (Fig. 7b). As observed in mice, human tissue samples with lower apical polarity scores had a significantly higher number of epithelial cell layers (Fig. 7c). To test for association between adipokines and apical polarity in normal breast tissue, we quantified *LEP* and *ADIPOQ* gene expression in the breast tissue samples. We chose this ratiometric assessment because the balance of adiponectin and leptin has been proposed to be critical in breast cancer initiation [40, 41], and because the adipokine ratio separated well normal vs. overweight/obese patient categories in the High Risk Duke cohort (Table 1 and Supplementary Fig. S7c). This

approach also reduced the impact of tissue sampling effects. As previously observed with circulating adipokines levels [11, 42], normal tissue from breast cancer patients had higher *LEP/ADIPOQ* transcript ratios compared to reduction mammoplasties (Supplementary Fig. S7d). We also found that tissue samples with high *LEP/ADIPOQ* transcript ratios had lower apical polarity as measured with ZO-1, Par3, and actin, or using a combination of the polarity markers (Fig. 7d-e).

Discussion

Apical-basal polarity is a hallmark of epithelial homeostasis [13, 15], and our results show that cellular microenvironments characteristic of obesity lead to mislocalization of apical polarity proteins in the mammary gland. A detrimental effect of obesity on cell-cell junctions has been documented in testes [43] and in the small intestine [44]. In both cases, chronic inflammation in obese tissue was shown to decrease TJ protein expression. In mammary acini produced in 3D culture, we found that elevated leptin levels are sufficient to disrupt apical polarity, as measured by altered localization of TJ, AJ, and PAR proteins, cortical actin remodeling, as well as increased permeability to small molecules. In our model, loss of apical marker localization was not accompanied by decreased polarity protein expression (Supplementary Fig. S8), but rather reflected subcellular relocalization of the proteins. Although we do not exclude that other stimuli may affect epithelial polarity in the mammary gland in the context of obesity, leptin-mediated loss of apical polarity in breast epithelial cells provides a mechanistic link between obesity or hyperleptinemia, and increased breast cancer risk (Fig. 6e).

Apical polarity is a gatekeeper architectural characteristic of normal epithelial tissue, and our experiments show that polarity loss in mammary acini has the detrimental functional consequences of sensitizing epithelial cells to growth-factor induced proliferation, deregulating mitotic spindle orientation, and expanding the pool of cells with stem/progenitor characteristics – all primordial events for cancer initiation. We measured a strong synergy between leptin, IGF-1 and insulin, which, in combination, caused cell cycle reentry. This effect can be explained in part by cross-talks between IGF-1R and LEPR [7] and by the up-regulation of LEPR expression by insulin [45]. In addition to synergies between the receptors, loss of apical polarity by leptin may alter the integration of proliferative signals from the microenvironment [46]. Our observation that sequential leptin and growth factor treatments induce Ki67 expression supports this hypothesis. In humans and a variety of species, circulating leptin and mammary leptin receptors increase dramatically during pregnancy and at the onset of puberty, which are critical phases of epithelial expansion. The importance of leptin as a permissive factor is further evident in leptin-deficient (ob/ob) mice that severely lack mammary ductal branching [47]. Hence, the potentiating functions of leptin in physiological conditions may go awry and prime cancer initiation in the context of obesity where the adipokine is at chronically high levels.

Mitotic spindle misorientation, which is likely not tumorigenic by itself, may promote cancer initiation in combination with other alterations to cellular homeostasis, such as proliferation and loss of anoikis. Cell divisions perpendicular to the basement membrane, as expected from a sub-population of cells exposed to elevated leptin in our experiments, is

indeed necessary (but not sufficient) for multilayering of the epithelium and may lead to the expansion of progenitor cells [48], which are currently recognized as initiators for basal-like tumors [49]. Interestingly, high leptin levels correlate with multilayering and hyperplasia [11], as well as with increased stem/progenitor cell self-renewal in normal breast tissue [39]. Moreover, we found higher proportions of cells with stem/progenitor characteristics in acini treated with leptin.

In mammary epithelial cells, leptin-mediated loss of apical polarity was caused by activation of PI3K/Akt signals by LEPR. Previously, PI3K inhibition was shown to promote phenotypic reversion of breast cancer cells in 3D culture, i.e. the reestablishment of polarity [50]. Conversely, delocalization of ZO-1 from cell-cell junctions and loss of claudins and occludins from TJ depend on PI3K/Akt signaling during epithelial to mesenchymal transition [51]. Akt regulates the remodeling of cortical actin [52], which is a key aspect of epithelial polarity. We therefore propose that over-activation of PI3K/Akt by leptin may alter mammary epithelial polarity by disrupting the cytoskeleton. In line with this hypothesis, remodeling of the actin cytoskeleton was observed in pancreatic β-cells and in vascular smooth muscles treated with leptin, and this effect was blocked by inhibiting PI3K activity [53]. Moreover, in our system, leptin treatment led to phosphorylation and redistribution of afadin, an Akt substrate and F-actin binding protein that regulates apical cell-cell junctions.

The PI3K/Akt pathway is activated early during (or likely prior to) breast carcinogenesis and plays an important role in the aggressive tumor biology, in particular for basal-like breast cancers characterized by rapid progression and a current lack of targeted therapies. Weight gain is associated with increased risk for premenopausal basal-like breast cancers [54]. Importantly, this cancer type disproportionally affects young African American women [55] for whom prevalence of overweight and obesity is the highest among the US adult population [56]. Our data establishing a role for leptin in cancer initiation are relevant for cancer prevention because leptin levels can be reduced by weight loss or pharmacologically with metformin. The findings pave the way for targeted chemoprevention based on epithelial polarity readouts, which may particularly benefit underserved populations.

Materials and Methods

Breast tissue procuration and analysis

Breast adipose and epithelial tissue were obtained following the Purdue Institutional Review Board protocol # 1206012467. Adipose tissue explants were either directly used in co-culture experiments or were used to generate conditioned medium. Histological assessment of the adipose tissue explants revealed minimal content of epithelium ($0.36\% \pm 0.15\%$) and confirmed viability. Breast tissue explants with epithelium were cryosectioned for immunostaining analyses. To measure interstitial tissue levels of cytokines, adipokines, and growth factors by ELISA, breast tissue obtained from a high-risk cohort [26] (under an Institutional Review Board-approved protocol at the Duke University Medical Center) were incubated short-term *ex-vivo*. Each BMI category was represented by n = 21 – 28 subjects. Additional information regarding human tissue procuration and analyses can be found in the Supplementary Materials and Methods.

Mice treatments and analyses

Female, four week old BALBc mice were placed on a low fat control diet (TD.08806) or on a lard-based obesity-inducing diet (60% kcal from fat; TD.06414), both from Envigo (Teklad diets, Indianapolis, IN, USA). Mammary glands were collected at 20 weeks of age, fixed, and embedded in paraffin. Immunohistochemistry was performed using Par3 (MilliporeSigma, Burlington MA, USA, 07–330, 2 μg/ml) and leptin (R&D Systems Minneapolis MN, USA, AF498, 2 μg/ml) antibodies. Tissue sections were stained with hematoxylin, and a Mantra system (Perkin Elmer, Waltham, MA, USA) was used for spectral imaging and channel separation of diaminobenzidine (DAB) and hematoxylin signals. Par3 localization was evaluated with a three-grade scale (0 = no apical signal; 1 = partial, discontinuous apical signal lining the lumen; 3 = continuous apical signal) by two investigators blind to the treatment conditions (25 acini or mammary ducts scored for each animal). Leptin signal intensity (DAB images after channel separation) was quantified in epithelial regions using ImageJ (https://imagej.nih.gov/ij/). Animal experimentation was done in compliance with ethical standards and was approved by the Animal Care and Use Committee of the Wake Forest School of Medicine (IACUC protocol #A16–010).

Cell culture

Non-neoplastic HMT-3522 S1 mammary epithelial cells [57] were cultured in 3D on top of a layer of Matrigel matrix (Corning, Corning NY, USA) as described [25]. Human mammary epithelial cells (post-stasis; psHMEC) were obtained from Lonza (Walkersville MD, USA) and cultured on Matrigel-coated surfaces with the supplier's Epithelial Cell Medium for up to 5 passages. Additional information regarding cell culture and treatments are provided in the Supplementary Materials and Methods.

Immunofluorescence

This procedure was performed as described previously [20]. Antibodies used are listed in Supplementary Materials and Methods. Actin was detected using SiR-actin (Cytoskeleton Inc., Denver CO USA, 0.25 μM, in live cells). Nuclei were counterstained with 4', 6-diamidino-2-phenylindole (DAPI) or with Hoechst 33342. Fixed samples were mounted in ProLong antifade solution (ThermoFisher, Waltham MA, USA). Confocal imaging was performed with a Zeiss (Oberkochen, Germany) CLSM710 confocal microscope, using a 63x oil immersion objective (NA = 1.4).

Quantification of apical polarity in 3D culture and human breast tissue

Fluorescent signals of polarity markers in 3D cell cultures were scored visually for apical localization using an Olympus IX83 microscope equipped with a 60x oil immersion objective (NA = 1.35). At least 100 acini were scored per condition in each experiment. For computer-based analysis of apical polarity, fluorescence images were taken with the CMOS camera (Hamamatsu, Bridgewater NJ, USA, ORCA-Flash4.0) on this microscope, using a 10x (NA = 0.3) objective. A custom ImageJ (http://rsbweb.nih.gov/ij/) script was used to extract acini from DAPI images and to calculate the radial distribution of the signals (see Supplementary Materials and Methods). 150–450 acini were analyzed per condition. Apical polarity in breast tissue sections was scored using a 4-grade system based on the presence

and continuity of staining at the apical membrane (0, < 20%; 1, 20–50%; 2, 50–80%, 3, 80–100%). The number of cell layers, defined as the maximum number of DAPI-stained nuclei along the basal-apical axis of the acinus or duct, was also recorded for each structure.

Western blot and qRT-PCR

Cells were lysed with 2% SDS in phosphate buffered saline. Protein concentrations were determined with the DC kit from BioRad (Hercules CA, USA). Equal amounts of proteins were resolved by SDS-PAGE, transferred onto nitrocellulose membranes for immunoblotting. The antibodies used are listed in Supplementary Material and Methods. For qRT-PCR analysis of leptin and adiponectin transcripts abundance in human breast tissue, RNA was extracted from tissue punches using the RNeasy Microarray Tissue Mini Kit (Qiagen, Hilden, Germany). cDNA synthesis and qPCR amplification were performed using the one-step Brilliant II SYBR Green QRT- PCR Master Mix Kit (Agilent, Santa Clara CA, USA). Absolute transcript abundance was quantified by generating standard curves, using target-specific gBlock gene fragments (IDT, Coralville IA, USA) as templates. Primer sequences are in Supplementary Material and Methods.

Statistical analysis

Statistical analysis was performed using Prism (GraphPad Software Inc., La Jolla CA, USA). Statistical tests are indicated with the corresponding P values in the figure legends. A P value < 0.05 was considered significant. All tests were two-sided. For the animal study, sample sizes were not based on power calculations since pre-specified effect sizes were not available.

Supplementary Material

Refer to Web version on PubMed Central for supplementary material.

Acknowledgements

References

1. Calle EE, Rodriguez C, Walker-Thurmond K, Thun MJ. Overweight, obesity, and mortality from cancer in a prospectively studied cohort of U.S. adults. The New England journal of medicine. 2003; 348: 1625–38. [PubMed: 12711737]

2. Renehan AG, Zwahlen M, Egger M. Adiposity and cancer risk: new mechanistic insights from epidemiology. Nature reviews Cancer. 2015; 15: 484–98. [PubMed: 26205341]

3. Schwartz GF, Hughes KS, Lynch HT, Fabian CJ, Fentiman IS, Robson ME, et al. Proceedings of the international consensus conference on breast cancer risk, genetics, & risk management, April, 2007. Cancer. 2008; 113: 2627–37. [PubMed: 18853415]

4. Cecchini RS, Costantino JP, Cauley JA, Cronin WM, Wickerham DL, Land SR, et al. Body mass index and the risk for developing invasive breast cancer among high-risk women in NSABP P-1 and

STAR breast cancer prevention trials. Cancer prevention research. 2012; 5: 583–92. [PubMed: 22318751]

5. Pierobon M, Frankenfeld CL. Obesity as a risk factor for triple-negative breast cancers: a systematic review and meta-analysis. Breast cancer research and treatment. 2013; 137: 307–14. [PubMed: 23179600]

6. Ando S, Catalano S. The multifactorial role of leptin in driving the breast cancer microenvironment. Nature reviews Endocrinology. 2012; 8: 263–75.

7. Saxena NK, Sharma D. Multifaceted leptin network: the molecular connection between obesity and breast cancer. Journal of mammary gland biology and neoplasia. 2013; 18: 309–20. [PubMed: 24214584]

8. Considine RV, Sinha MK, Heiman ML, Kriauciunas A, Stephens TW, Nyce MR, et al. Serum immunoreactive-leptin concentrations in normal-weight and obese humans. The New England journal of medicine. 1996; 334: 292–5. [PubMed: 8532024]

9. Matsubara M, Maruoka S, Katayose S. Inverse relationship between plasma adiponectin and leptin concentrations in normal-weight and obese women. European journal of endocrinology / European Federation of Endocrine Societies. 2002; 147: 173–80.

10. Wheatley KE, Nogueira LM, Perkins SN, Hursting SD. Differential effects of calorie restriction and exercise on the adipose transcriptome in diet-induced obese mice. Journal of obesity. 2011; 2011: 265417. [PubMed: 21603264]

11. Niu J, Jiang L, Guo W, Shao L, Liu Y, Wang L. The Association between Leptin Level and Breast Cancer: A Meta-Analysis. PloS one. 2013; 8: e67349. [PubMed: 23826274]

12. Wu MH, Chou YC, Chou WY, Hsu GC, Chu CH, Yu CP, et al. Circulating levels of leptin, adiposity and breast cancer risk. British journal of cancer. 2009; 100: 578–82. [PubMed: 19223908]

13. Lelievre SA. Tissue polarity-dependent control of mammary epithelial homeostasis and cancer development: an epigenetic perspective. Journal of mammary gland biology and neoplasia. 2010; 15: 49–63. [PubMed: 20101444]

14. Royer C, Lu X. Epithelial cell polarity: a major gatekeeper against cancer? Cell Death Differ. 2011; 18: 1470–7. [PubMed: 21617693]

15. Martin-Belmonte F, Perez-Moreno M. Epithelial cell polarity, stem cells and cancer. Nature reviews Cancer. 2012; 12: 23–38.

16. Balda MS, Matter K. The tight junction protein ZO-1 and an interacting transcription factor regulate ErbB-2 expression. The EMBO journal. 2000; 19: 2024–33. [PubMed: 10790369]

17. Feigin ME, Akshinthala SD, Araki K, Rosenberg AZ, Muthuswamy LB, Martin B, et al. Mislocalization of the cell polarity protein scribble promotes mammary tumorigenesis and is associated with basal breast cancer. Cancer Res. 2014; 74: 3180–94. [PubMed: 24662921]

18. Fang L, Wang Y, Du D, Yang G, Tak Kwok T, Kai Kong S, et al. Cell polarity protein Par3 complexes with DNA-PK via Ku70 and regulates DNA double-strand break repair. Cell research. 2007; 17: 100–16. [PubMed: 17287830]

19. Chandramouly G, Abad PC, Knowles DW, Lelievre SA. The control of tissue architecture over nuclear organization is crucial for epithelial cell fate. Journal of cell science. 2007; 120: 1596–606. [PubMed: 17405811]

20. Vidi PA, Chandramouly G, Gray M, Wang L, Liu E, Kim JJ, et al. Interconnected contribution of tissue morphogenesis and the nuclear protein NuMA to the DNA damage response. Journal of cell science. 2012; 125: 350–61. [PubMed: 22331358]

21. Sumis A, Cook KL, Andrade FO, Hu R, Kidney E, Zhang X, et al. Social isolation induces autophagy in the mouse mammary gland: link to increased mammary cancer risk. Endocrine-related cancer. 2016; 23: 839–56. [PubMed: 27550962]

22. Roignot J, Peng X, Mostov K. Polarity in mammalian epithelial morphogenesis. Cold Spring Harbor perspectives in biology. 2013; 5.

23. McCaffrey LM, Montalbano J, Mihai C, Macara IG. Loss of the Par3 polarity protein promotes breast tumorigenesis and metastasis. Cancer cell. 2012; 22: 601–14. [PubMed: 23153534]

24. Petersen OW, Ronnov-Jessen L, Howlett AR, Bissell MJ. Interaction with basement membrane serves to rapidly distinguish growth and differentiation pattern of normal and malignant human breast epithelial cells. Proc Natl Acad Sci U S A. 1992; 89: 9064–8. [PubMed: 1384042]

25. Vidi PA, Bissell MJ, Lelievre SA. Three-dimensional culture of human breast epithelial cells: the how and the why. Methods in molecular biology. 2013; 945: 193–219. [PubMed: 23097109]

26. Ibarra-Drendall C, Troch MM, Barry WT, Broadwater G, Petricoin EF 3rd, Wulfkuhle J, et al. Pilot and feasibility study: prospective proteomic profiling of mammary epithelial cells from high-risk women provides evidence of activation of pro-survival pathways. Breast cancer research and treatment. 2012; 132: 487–98. [PubMed: 21647677]

27. Gunter MJ, Hoover DR, Yu H, Wassertheil-Smoller S, Rohan TE, Manson JE, et al. Insulin, insulin-like growth factor-I, and risk of breast cancer in postmenopausal women. Journal of the National Cancer Institute. 2009; 101: 48–60. [PubMed: 19116382]

28. Kim CS, Park HS, Kawada T, Kim JH, Lim D, Hubbard NE, et al. Circulating levels of MCP-1 and IL-8 are elevated in human obese subjects and associated with obesity-related parameters. International journal of obesity. 2006; 30: 1347–55. [PubMed: 16534530]

29. Carpenter RL, Paw I, Dewhirst MW, Lo HW. Akt phosphorylates and activates HSF-1 independent of heat shock, leading to Slug overexpression and epithelial-mesenchymal transition (EMT) of HER2-overexpressing breast cancer cells. Oncogene. 2015; 34: 546–57. [PubMed: 24469056]

30. Elloul S, Kedrin D, Knoblauch NW, Beck AH, Toker A. The adherens junction protein afadin is an AKT substrate that regulates breast cancer cell migration. Molecular cancer research : MCR. 2014; 12: 464–76. [PubMed: 24269953]

31. Takai Y, Ikeda W, Ogita H, Rikitake Y. The immunoglobulin-like cell adhesion molecule nectin and its associated protein afadin. Annual review of cell and developmental biology. 2008; 24: 309–42.

32. Ooshio T, Kobayashi R, Ikeda W, Miyata M, Fukumoto Y, Matsuzawa N, et al. Involvement of the interaction of afadin with ZO-1 in the formation of tight junctions in Madin-Darby canine kidney cells. The Journal of biological chemistry. 2010; 285: 5003–12. [PubMed: 20008323]

33. Dubois V, Jarde T, Delort L, Billard H, Bernard-Gallon D, Berger E, et al. Leptin induces a proliferative response in breast cancer cells but not in normal breast cells. Nutrition and cancer. 2014; 66: 645–55. [PubMed: 24738610]

34. Ray A, Cleary MP. The potential role of leptin in tumor invasion and metastasis. Cytokine Growth Factor Rev. 2017; 38: 80–97. [PubMed: 29158066]

35. Macara IG, Guyer R, Richardson G, Huo Y, Ahmed SM. Epithelial homeostasis. Current biology : CB. 2014; 24: R815–25. [PubMed: 25202877]

36. Hao Y, Du Q, Chen X, Zheng Z, Balsbaugh JL, Maitra S, et al. Par3 controls epithelial spindle orientation by aPKC-mediated phosphorylation of apical Pins. Current biology : CB. 2010; 20: 1809–18. [PubMed: 20933426]

37. Carminati M, Gallini S, Pirovano L, Alfieri A, Bisi S, Mapelli M. Concomitant binding of Afadin to LGN and F-actin directs planar spindle orientation. Nat Struct Mol Biol. 2016; 23: 155–63. [PubMed: 26751642]

38. Grafton MM, Wang L, Vidi PA, Leary J, Lelievre SA. Breast on-a-chip: mimicry of the channeling system of the breast for development of theranostics. Integrative biology : quantitative biosciences from nano to macro. 2011; 3: 451–9. [PubMed: 21234506]

39. Esper RM, Dame M, McClintock S, Holt PR, Dannenberg AJ, Wicha MS, et al. Leptin and Adiponectin Modulate the Self-renewal of Normal Human Breast Epithelial Stem Cells. Cancer prevention research. 2015; 8: 1174–83. [PubMed: 26487401]

40. Hursting SD, Digiovanni J, Dannenberg AJ, Azrad M, Leroith D, Demark-Wahnefried W, et al. Obesity, energy balance, and cancer: new opportunities for prevention. Cancer prevention research. 2012; 5: 1260–72. [PubMed: 23034147]

41. Grossmann ME, Cleary MP. The balance between leptin and adiponectin in the control of carcinogenesis - focus on mammary tumorigenesis. Biochimie. 2012; 94: 2164–71. [PubMed: 22728769]

42. Macis D, Guerrieri-Gonzaga A, Gandini S. Circulating adiponectin and breast cancer risk: a systematic review and meta-analysis. International journal of epidemiology. 2014; 43: 1226–36. [PubMed: 24737805]

43. Fan Y, Liu Y, Xue K, Gu G, Fan W, Xu Y, et al. Diet-induced obesity in male C57BL/6 mice decreases fertility as a consequence of disrupted blood-testis barrier. PloS one. 2015; 10: e0120775. [PubMed: 25886196]

44. Teixeira TF, Collado MC, Ferreira CL, Bressan J, Peluzio Mdo C. Potential mechanisms for the emerging link between obesity and increased intestinal permeability. Nutrition research. 2012; 32: 637–47. [PubMed: 23084636]

45. Bartella V, Cascio S, Fiorio E, Auriemma A, Russo A, Surmacz E. Insulin-dependent leptin expression in breast cancer cells. Cancer Res. 2008; 68: 4919–27. [PubMed: 18559540]

46. Bissell MJ, Weaver VM, Lelievre SA, Wang F, Petersen OW, Schmeichel KL. Tissue structure, nuclear organization, and gene expression in normal and malignant breast. Cancer Res. 1999; 59: 1757–1763s; discussion 1763s-1764s. [PubMed: 10197593]

47. Hu X, Juneja SC, Maihle NJ, Cleary MP. Leptin--a growth factor in normal and malignant breast cells and for normal mammary gland development. Journal of the National Cancer Institute. 2002; 94: 1704–11. [PubMed: 12441326]

48. Martin-Belmonte F, Gassama A, Datta A, Yu W, Rescher U, Gerke V, et al. PTEN-mediated apical segregation of phosphoinositides controls epithelial morphogenesis through Cdc42. Cell. 2007; 128: 383–97. [PubMed: 17254974]

49. Rangel MC, Bertolette D, Castro NP, Klauzinska M, Cuttitta F, Salomon DS. Developmental signaling pathways regulating mammary stem cells and contributing to the etiology of triple-negative breast cancer. Breast cancer research and treatment. 2016; 156: 211–26. [PubMed: 26968398]

50. Wang F, Hansen RK, Radisky D, Yoneda T, Barcellos-Hoff MH, Petersen OW, et al. Phenotypic reversion or death of cancer cells by altering signaling pathways in three-dimensional contexts. Journal of the National Cancer Institute. 2002; 94: 1494–503. [PubMed: 12359858]

51. Bakin AV, Tomlinson AK, Bhowmick NA, Moses HL, Arteaga CL. Phosphatidylinositol 3-kinase function is required for transforming growth factor beta-mediated epithelial to mesenchymal transition and cell migration. The Journal of biological chemistry. 2000; 275: 36803–10. [PubMed: 10969078]

52. Xue G, Hemmings BA. PKB/Akt-dependent regulation of cell motility. Journal of the National Cancer Institute. 2013; 105: 393–404. [PubMed: 23355761]

53. Zeidan A, Paylor B, Steinhoff KJ, Javadov S, Rajapurohitam V, Chakrabarti S, et al. Actin cytoskeleton dynamics promotes leptin-induced vascular smooth muscle hypertrophy via RhoA/ROCK- and phosphatidylinositol 3-kinase/protein kinase B-dependent pathways. The Journal of pharmacology and experimental therapeutics. 2007; 322: 1110–6. [PubMed: 17562852]

54. Millikan RC, Newman B, Tse CK, Moorman PG, Conway K, Dressler LG, et al. Epidemiology of basal-like breast cancer. Breast cancer research and treatment. 2008; 109: 123–39. [PubMed: 17578664]

55. Dietze EC, Sistrunk C, Miranda-Carboni G, O'Regan R, Seewaldt VL. Triple-negative breast cancer in African-American women: disparities versus biology. Nature reviews Cancer. 2015; 15: 248–54. [PubMed: 25673085]

56. Ogden CL, Carroll MD, Fryar CD, Flegal KM. Prevalence of Obesity Among Adults and Youth: United States, 2011–2014. NCHS data brief. 2015; 1–8.

57. Briand P, Petersen OW, Van Deurs B. A new diploid nontumorigenic human breast epithelial cell line isolated and propagated in chemically defined medium. In Vitro Cell Dev Biol. 1987; 23: 181–8. [PubMed: 3558253]
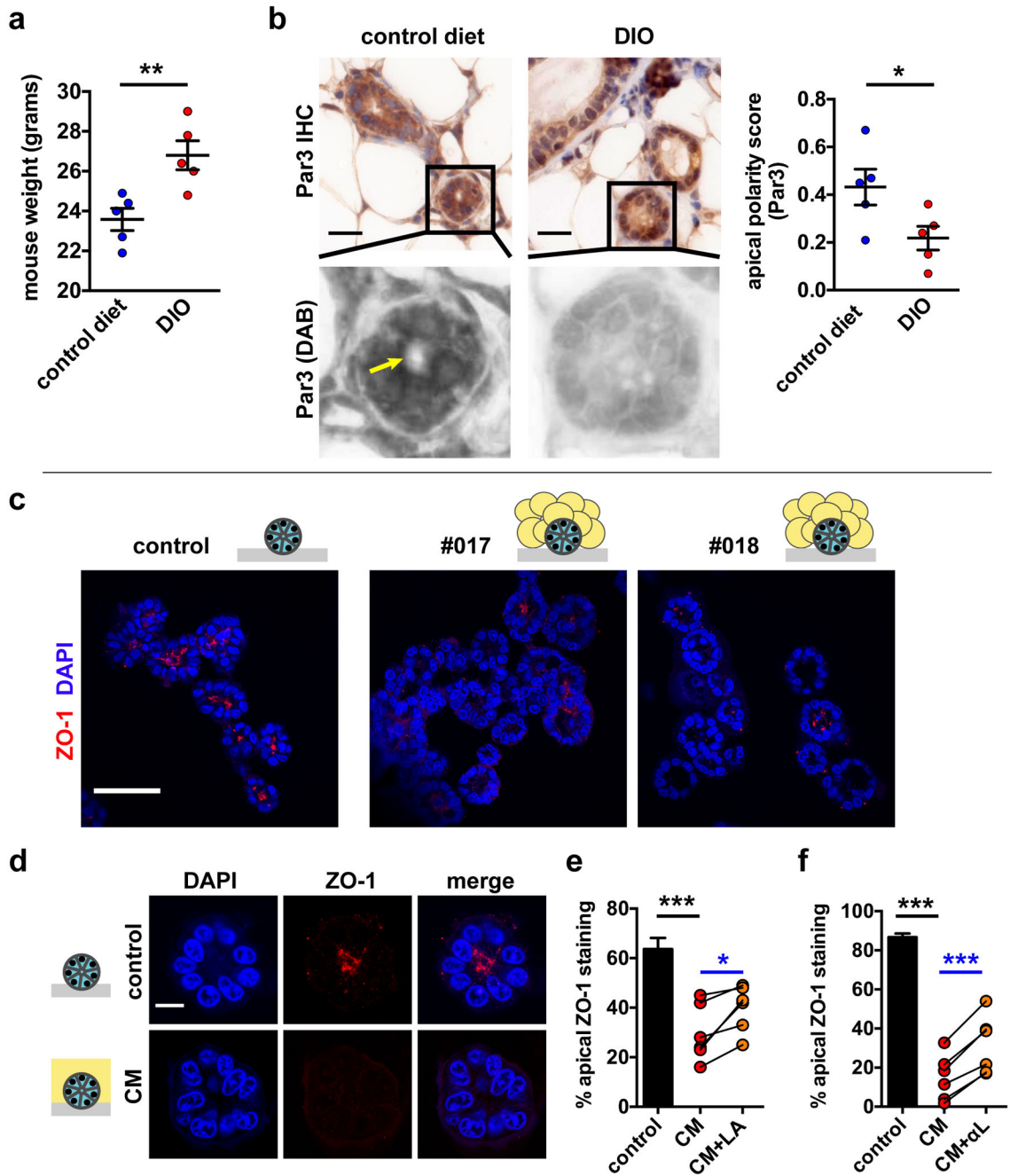
Fig. 1.

Loss of apical polarity in mouse and 3D cell culture models of obesity. **a** Weight gain in BALB/c mice fed a high-fat diet (DIO) for 16 weeks compared to littermates fed a control chow diet. **, $P < 0.01$ (unpaired t-test, n = 5). **b** Analysis of the Par3 apical marker distribution in whole mount mammary glands from DIO mice and controls. Spectral imaging was used to separate immunohistochemical signals (DAB). The arrow indicates apical Par3 localization. Quantification of Par3 localization is shown in the bar graph. *, $P < 0.05$ (unpaired t-test, n = 5). **c** Detection of the tight junction marker ZO-1 by immunostaining and confocal microscopy in HMT-3522 S1 breast acini in 3D cell culture. Differentiated

acini were cultured in isolation (control) or cocultured for three days with adipose tissue explants derived from reduction mammoplasties (patients #017 and #018). Nuclei were counterstained with DAPI. **d** ZO-1 distribution in S1 acini treated for 3 days with medium conditioned by human mammary adipose (CM). **e-f** Quantification of ZO-1 localization in untreated acini (control) and in acini treated with CM, in the absence or presence of a LEPR antagonist (LA; 1 μg/ml) **(e)** or leptin neutralizing antibodies (αL) **(f)**. CM was generated with adipose tissue from different patients, each represented by a dot on the graphs. *, $P <$ 0.05 and ***, $P < 0.001$ (unpaired t-test [black] or paired t-test [blue]; n = 6). Means ± SEM are shown in the graphs. Scale bars, 20 μm **(b)**, 50 μm **(c)**, and 10 μm **(d)**.
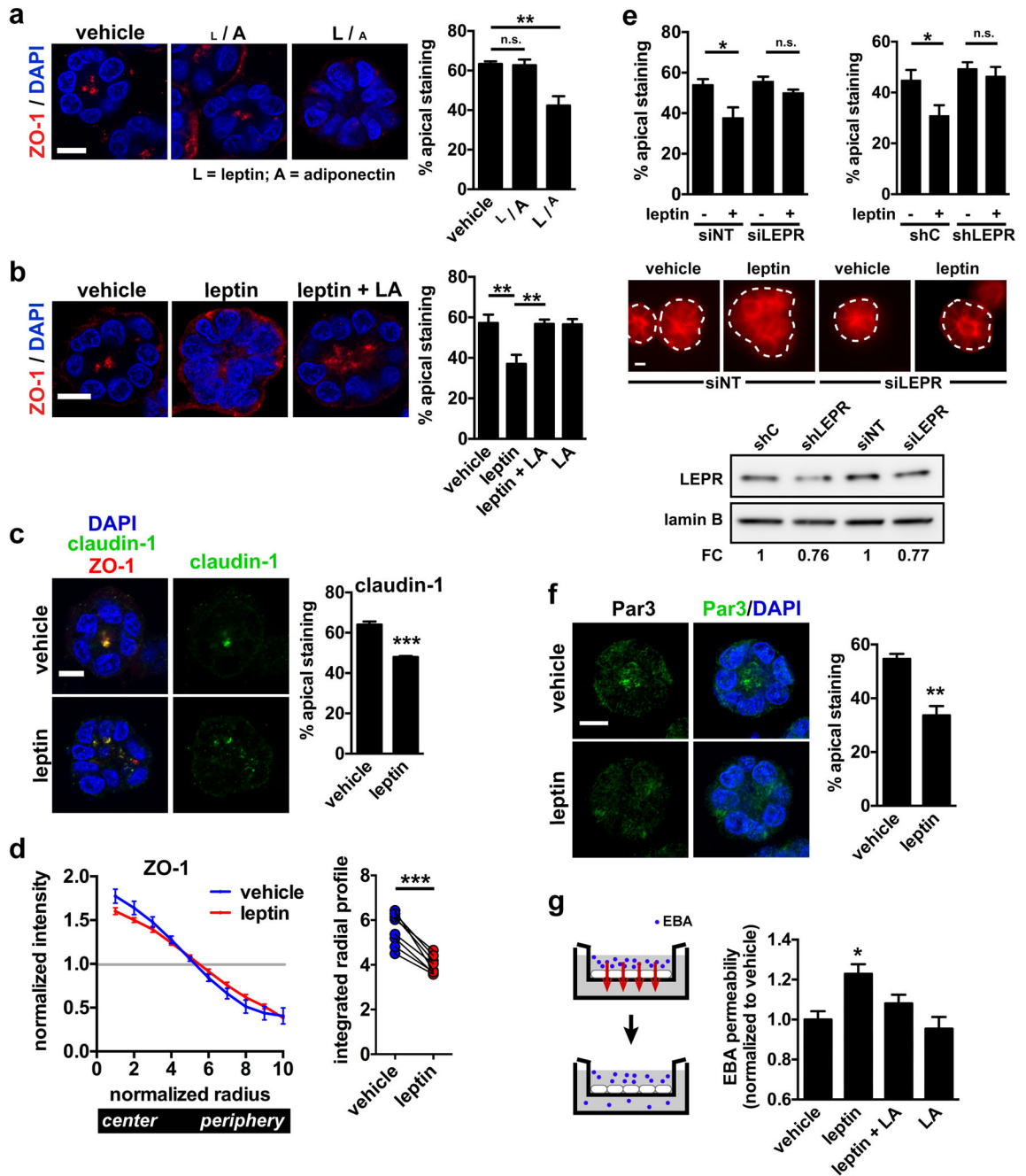
Fig 2.

Disruption of apical polarity by leptin. **a** Confocal images of ZO-1 staining in S1 acini treated for 72h with vehicle or with low or high leptin/adiponectin ratios (^{L} / A and L / ^{A}, respectively). [^{L} / A], 10 ng/ml leptin and 10 μg/ml adiponectin; [L / ^{A}], 100 ng/ml leptin and 0.1 μg/ml adiponectin. Nuclei were counterstained with DAPI. Quantification of the percentages of acini with apical ZO-1 localization is shown in the bar graph. **, $P < 0.01$ (one-way ANOVA and Tukey's post-hoc test; n = 3). **b** Immunostaining for ZO-1 in differentiated S1 acini treated for 72h with vehicle, with leptin (100 ng/ml), or with leptin and LEPR antagonist (LA). Representative confocal images and quantification of apical

marker distribution are shown. **, *P* < 0.01 (one-way ANOVA and Tukey's post-hoc test; n = 5). **c** Localization of claudin-1 in acini treated for 72h with leptin or vehicle. Dual staining with ZO-1 shows overlap between the two TJ markers. ***, *P* < 0.001 (unpaired t-test; n = 3). **d** Averaged radial profiles (RP) of ZO-1 staining in S1 acini treated with vehicle of leptin (n = 8 biological replicates). The curves represent normalized staining intensity along the radii of the structures. Integrated values of RP curves are shown on the right. To obtain these values, 1.0 was subtracted from the normalized intensity of each radii bins (bin 1 at the center to bin 10 at the periphery), and absolute values were summed. ***, *P* < 0.0001 (paired t-test, n = 8). **e** Cortical actin labeling in live S1 acini. Cells were nucleofected with nontargeting (NT) and LEPR-specific siRNA (left), or with scrambled shRNA (shC) and LEPR shRNA (right) before treatment with vehicle or leptin (24h; 100 ng/ml). Each nucleofection reaction included plasmid DNA encoding GFP to guide the analysis. *, *P* < 0.05 (one-way ANOVA and Tukey's post-hoc test; n = 3). Representative images of acini nucleofected with siNT and siLEPR are shown. The dotted lines represent the outlines of the acini (based on DAPI signals). LEPR silencing (siRNA and shRNA nucleofections) was verified by western blot. *Note* that the 20% reduction in LEPR expression mirrors the proportion of GFP-positive acini in these experiments, suggesting efficacious LEPR silencing in the cells that were successfully nucleofected with si- and shLEPR. **f** Localization of Par3 in acini treated for 72h with leptin or vehicle. **, *P* < 0.01 (unpaired t-test; n = 3). **g** Transepithelial permeability to Evans blue albumin (EBA) in S1 cell monolayers treated as in C. *, *P* < 0.05 (compared to all other treatments, one-way ANOVA and Fisher's LSD, n = 8 measurements from 3 biological replicates). Means ± SEM are shown in the graphs. Scale bars, 10 μm.
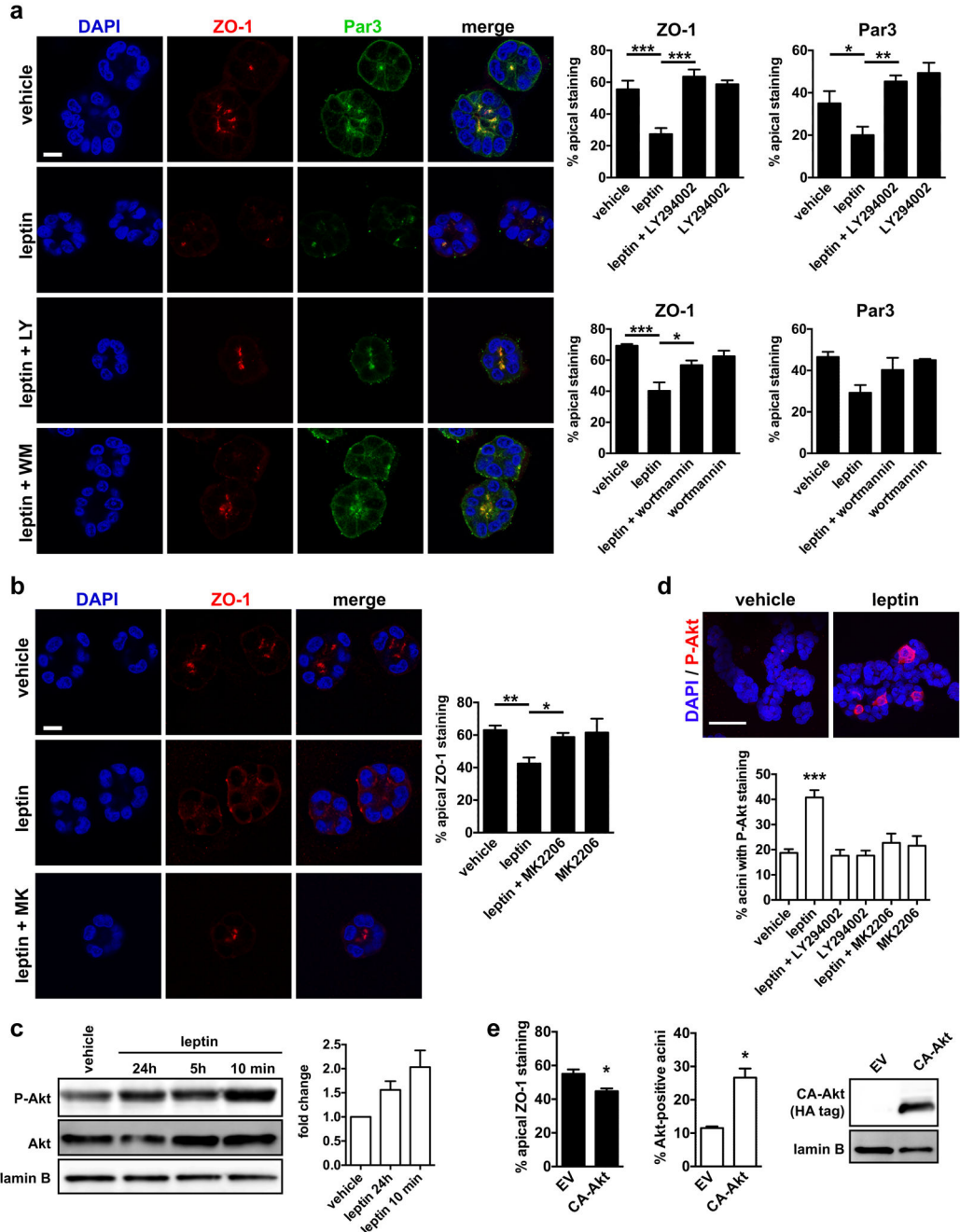
Fig. 3.
The PI3K pathway mediates apical polarity loss by leptin. **a** Localization of apical polarity markers ZO-1 and Par3 in S1 acini treated for 72h with vehicle or leptin (100 ng/ml) in the presence or absence of the PI3K inhibitors LY294002 (LY; 8 µM) or wortmannin (WM; 1 µM). Quantification of the percentages of acini with apical ZO-1 and Par3 localization is shown in the graphs. *, $P < 0.05$; **, $P < 0.01$; ***, $P < 0.001$ (one-way ANOVA and Tukey's; n = 3–5). **b** Apical ZO-1 distribution in acini treated with leptin and the Akt inhibitors MK2206 (MK; 10 µM). *, $P < 0.05$; **, $P < 0.01$ (one-way ANOVA and Tukey's; n = 4). **c** Western blot analysis of S1 monolayer extracts to verify PI3K pathway activation

by leptin. Average fold changes were calculated by densitometry and are shown in the bar graph (n = 3, mean ± SEM). **d** Top: Detection of P-Akt by immunostaining in S1 acini treated with vehicle or with leptin (24h). Bottom: Quantification of P-Akt-positive acini after treatment with vehicle or leptin, in the presence or absence of LY and MK. ***, $P < 0.001$ (compared to all other treatments, one-way ANOVA and Fisher's LSD, n = 3). **e** Apical ZO-1 localization and Akt staining in acini derived from S1 cell transfected with constitutively activated Akt (CA-Akt) or with empty vector (EV). *, $P < 0.05$ (unpaired t-test; n = 3). CA-Akt expression was verified by western blot. Lamin B is shown as loading control. Means ± SEM are shown in the graphs. Scale bars, 10 μm (a, b) and 50 μm (c).
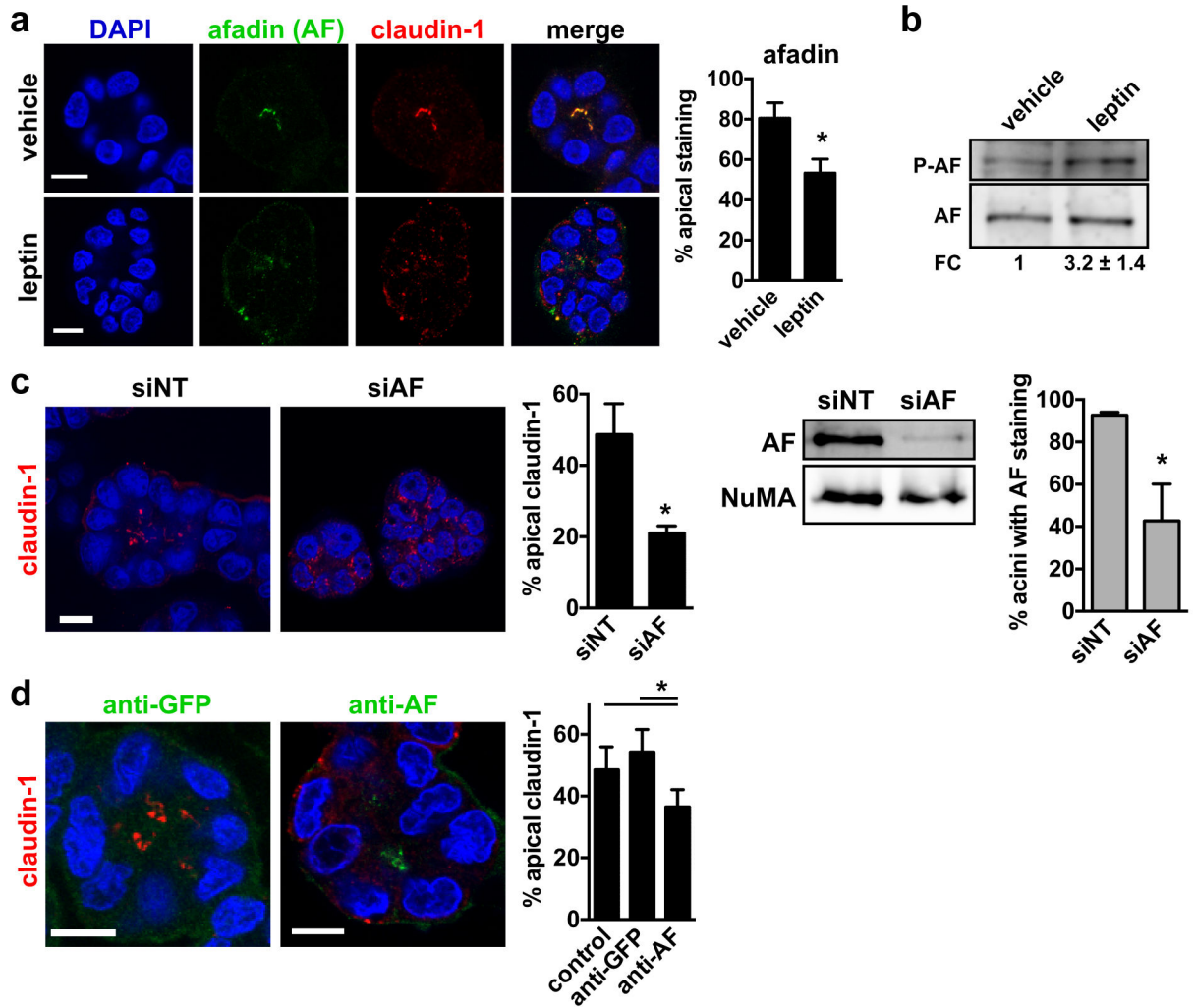
Fig. 4.

Leptin leads to mislocalization of the Akt substrate afadin. **a** Immunostaining for afadin (AF) and claudin-1 in differentiated S1 acini treated for 72h with vehicle or leptin (100 ng/ml). The proportion of acini with apical AF is shown on the graph. *, $P < 0.05$ (unpaired t-test; n = 3). **b** Western blot analysis of total and phosphorylated AF (S1718) in S1 cells treated with vehicle or leptin. Fold change (FC) was calculated by densitometry (n = 3). **c** Quantification of apical claudin-1 localization in acini derived from S1 cells transfected with nontargeting (NT) or AF-specific siRNA. *, $P < 0.05$ (unpaired t-test; n = 3). AF silencing was verified by western blot in 2D S1 cultures used for seeding 3D acini cultures. NuMA is shown as loading control. AF silencing was also verified by immunostaining in S1 acini. The proportion of acini with detectable AF signals is shown on the right. *, $P < 0.05$; (unpaired t-test; n = 3). **d** Introduction of AF antibodies in live S1 acini. Acini were fixed after 2h incubation with anti-AF or anti-GFP (used as control). Claudin-1 was localized by immunofluorescence. Afadin and GFP antibodies were visualized using secondary fluorescent antibodies. The proportion of acini with apical claudin-1 are shown. *, $P < 0.05$ (one-way ANOVA and Tukey's, n = 4). Mean ± SEM are shown in the graphs. Scale bars, 10 μm.
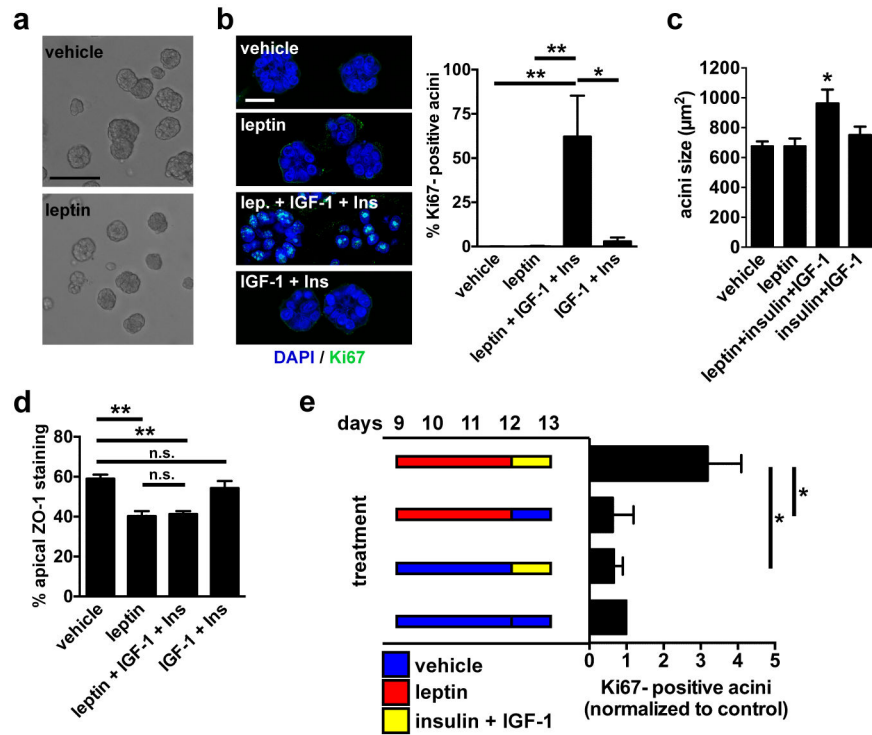
Fig. 5.

Leptin primes mammary epithelial cells for proliferation. **a** Bright field micrographs of differentiated S1 acini treated for 72h with vehicle or leptin. Scale bar, 100 μm. **b** Representative confocal images and quantification of Ki67 staining in acini treated for 72h with vehicle, with leptin (100 ng/ml), with IGF-1 (0.1 μg/ml) and elevated insulin (500 ng/ml), or with the combination of the three factors. Scale bar, 20 μm. *, $P < 0.05$ and **, $P < 0.01$ (one-way ANOVA and Tukey's; n = 5). **c** Sizes (cross sections) of acini treated as in B. *, $P < 0.05$ (compared to all other treatments, one-way ANOVA and Fisher's LSD, n = 3). **d** Apical localization of ZO-1 in acini treated as in B. **, $P < 0.01$, n.s., $P > 0.05$ (one-way ANOVA and Tukey's; n = 3). **e** Analysis of Ki67 in S1 acini after treatments with leptin and growth factors. Treatments were dissociated in time, as indicated in the schematic. Values were normalized to control (vehicle/vehicle). *, $P < 0.05$ (Kruskal-Wallis and Dunn's, n = 4).
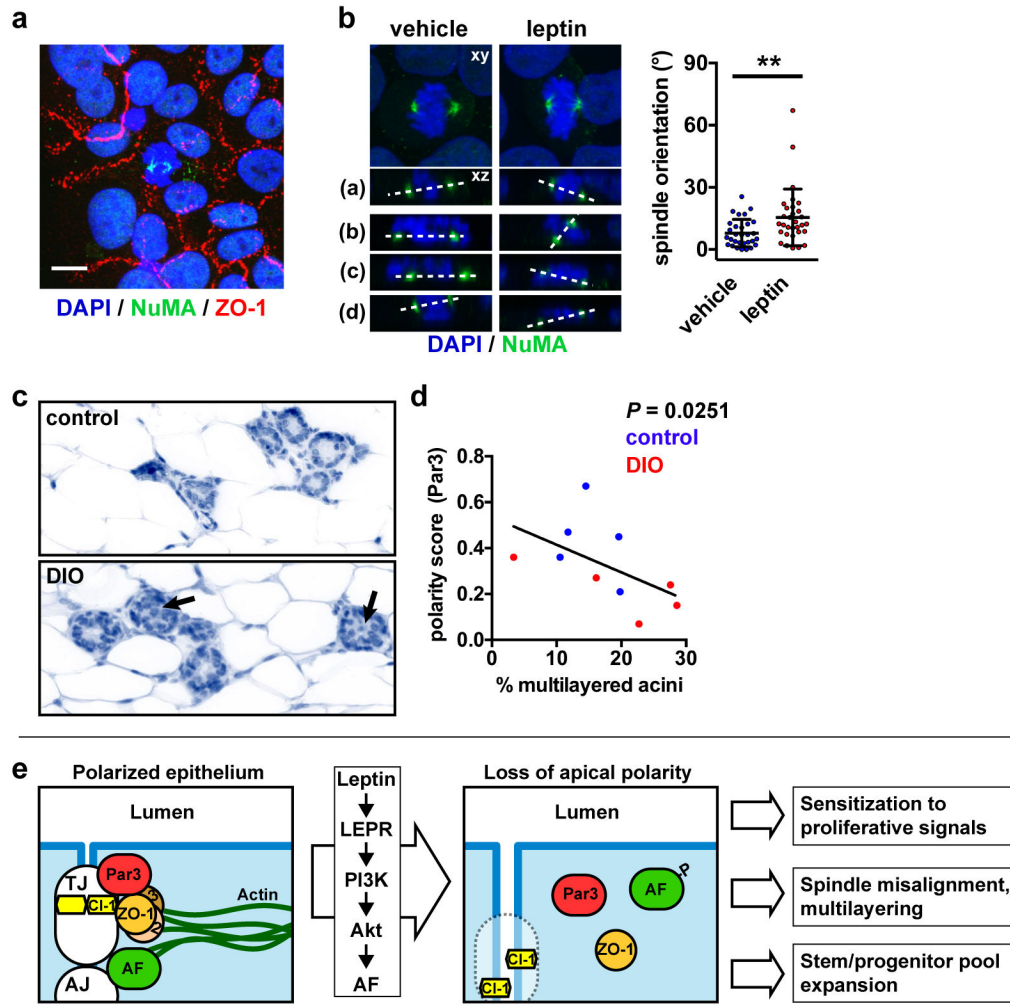
Fig. 6.

Leptin leads to mitotic spindle misalignment. **a** Detection of ZO-1 and NuMA by immunofluorescence in polarized monolayers of S1 cells. Scale bar, 10 μm. **b** Mitotic spindle orientation in S1 cell monolayers treated with vehicle or leptin, as measured by confocal microscopy. Images on top represent maximal intensity projections whereas bottom images (a-d) are representative orthogonal views of the dual NuMA-DAPI staining. Angles between the two spindle poles (dashed lines) and the horizontal are quantified in the graph. **, $P < 0.01$ (unpaired t-test, n = 30 cells from two independent experiments). **c** Histology of mammary glands from mice with diet-induced obesity (DIO) and mice fed a control diet. Arrows indicate multilayered acini, defined as having ≥ 3 cell layers. **d** Correlation between apical polarization (Par3 score) and multilayering in the mammary epithelium from control and DIO mice. The exact *P* value (two-tailed Spearman test) was computed. The graphs represent mean ± SEM (B-E) or mean ± SD (G). **e** Schematic summarizing the effect of leptin on epithelial polarity and the functional consequences of polarity loss in the premalignant context.
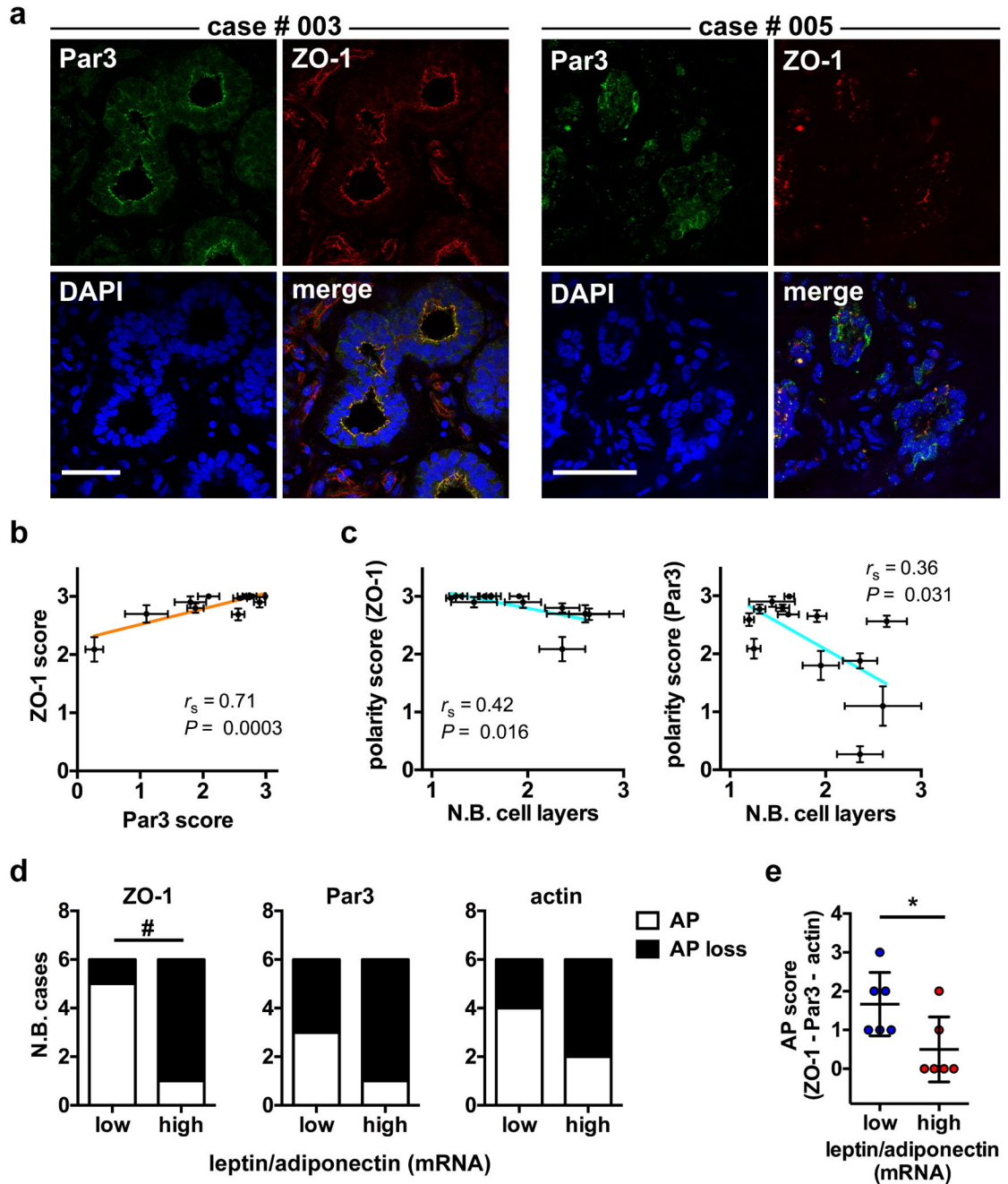
Fig. 7.
Apical polarity correlates with epithelial multilayering and adipokine imbalance in human breast tissue. **a** Confocal microscopy images of ZO-1 and Par3 immunostaining in frozen sections from normal breast tissue from two different patients (003 and 005). Cell nuclei were conterstained with DAPI. Scale bars, 50 μm. **b** Association between apical polarity scores derived from ZO-1 and Par3 staining. The Pearson correlation coefficient (r_s) and P value are shown. Each dot on the graph represents one patient (n = 13). Error bars are SEM. **c** Association between apical polarity scores (ZO-1 or Par3) and the number of epithelial cell layers, determined based on DAPI images. Mean ± SEM are shown for each patient (n = 13)

with r_s and P values. **d-e** Apical polarity in normal breast tissue classified based on their relative leptin/adiponectin transcript abundance (high, above median; low, below median). Apical polarity (AP) loss was defined as patient score averages below the 25th percentile (ZO-1 and Par3) or below the 50th percentile (actin). AP results for ZO-1, Par3, and actin are shown individually (**d**) or in combination, by adding scores values of each marker (**e**; mean ± SD). #, $P < 0.05$ (two tailed Chi-square test); *, $P < 0.05$ (two tailed Mann-Whitney test).

Table 1.

Tissue levels of adipokines, cytokines and growth factors by BMI categories.

Variable	Normal weight	Overweight	Obese	Spearman correlation coefficient
BMI	21.9 ± 2.0	27.0 ± 1.4	32.5 ± 3.7	
Adiponectin	1.41E+07 ± 9.54E+06	1.33E+07 ± 1.13E+07	1.37E+07 ± 1.62E+07	−0.156
NGF	12.7 ± 5.8	14.8 ± 7.3	13.2 ± 3.8	−0.091
IL-6	7.8 ± 6.4	7.2 ± 7.6	6.6 ± 3.6	−0.011
Insulin	601 ± 591	861 ± 1267	8178 ± 544	0.124
Leptin [###]	11 899 ± 9668	22 117 ± 15 235	27 799 ± 10 628	0.576 [*]
IL-8	2.0 ± 1.5	1.8 ± 0.9	1.7 ± 0.9	−0.059
HGF	195 ± 114	252 ± 169	195 ± 181	−0.086
MCP-1	141 ± 106	158 ± 107	172 ± 166	0.028
TNFα [#]	2.4 ± 0.8	2.8 ± 0.9	2.6 ± 1.4	−0.117
IL-1β	3.9 ± 4.5	3.6 ± 3.6	2.8 ± 2.0	−0.086
TGFβ	21 898 ± 16 239	24 888 ± 11 350	20 561 ± 12 130	0.077
Masood Score	14.9 ± 1.5	13.6 ± 2.2	13.6 ± 2.2	
A/L ratio [#]	7283 ± 5316	479 ± 488	701 ± 1214	0.104

All values are in ng/g tissue and represent mean ± SD. The body-mass index (BMI) is defined as the weight (kg) divided by the square of the height (m). BMI categories are: 18.5-24.9, normal weight; 25-29.9, overweight; 30, obese. A/L, adiponectin/leptin.

Spearman correlation is between adipokine/cytokine/growth factor levels and BMI.

[*]$P < 0.0001$.

[#,]$P < 0.05$ and

[###,]$P < 0.001$ (two-sided Kruskal-Wallis test). n = 50 (adiponectin) or 74 (all others).